Effects of Rotor Skew on the Performance of Brushless Doubly-Fed Induction Machine

Xuezhou Wang, Tim D. Strous, Domenico Lahaye, Henk Polinder, *Senior Member, IEEE,*
Jan A. Ferreira, *Fellow, IEEE*

***Abstract*—Brushless doubly-fed induction machines (BDFIM) have great potential as variable-speed generators in larger-scale wind turbines. Undesired space harmonics exist because the special rotor needs to couple both two stator windings which with different pole-pair numbers and different frequencies. These rich space harmonics lead to a bigger torque ripple comparing to the normal induction machine. This paper makes use of 2D multi-slice finite element (FE) method to study the effect of the rotor skew on the performance of the BDFIM in the cases without and with saturation. The results show the torque ripple is reduced significantly by skewing the rotor both in those two situations. But the rotor skew has negligible influence on the harmonics due to the saturation effect. Furthermore, the rotor skew has little influence on the total amount of losses. However, based on the simulation results, it redistributes the core losses along the axial direction in the BDFIM.**

***Index Terms*—Brushless, cross-coupling, doubly-fed, finite element analysis, induction machine, multi-slice method, nested-loop rotor, skewing effect, torque ripple.**

I. Introduction

THE brushless doubly-fed induction machine (BDFIM) came from the idea of self-cascaded machine in 1903. The modern BDFIM has two stator AC supplies with different pole-pairs to avoid their direct magnetic coupling. The magnetic coupling is achieved through a special rotor like Fig. 1. Fig. 2 shows a typical structure of BDFIM. One of the stator windings is referred as the power winding which is connected with the grid directly. The other one is called as the control winding which is connected to the grid through a partially rated converter giving a variable frequency and voltage. This configure makes the BDFIM operate at variable speed with respect to the wind speeds, like a doubly-fed induction machine (DFIM) which is currently the most common generator for wind turbines [1]. Furthermore, the BDFIM has some additional advantages comparing with the commonly applied DFIM including:

- The reliability is improved by eliminating the brush and the slip rings. Therefore, the maintenance cost of the generator will decrease [2].
- A better fault ride-through capability [3].
- The BDFIM can be a medium-speed generator so that one or two-stage gearbox can be utilized. Then the capital cost will reduce while a higher reliability can be achieved [4].

Considering its benefits, the BDFIM has great potential as a new generator in large-scale wind turbines [5], especially for off-shore installations. However, on the other hand, the BDFIM also has some disadvantages such as higher manufacturing cost, a slightly larger dimension and lower efficiency comparing with DFIM with same rating [6].

The air-gap contains two main magnetic fields (created by the power winding and the control winding) with different pole-pair numbers and different frequencies. The special nested-loop rotor is designed to couple with both two main harmonic field resulting in a complex distribution of the magnetic field in this special machine [7]. The undesirable space harmonics are mainly responsible for the previous drawbacks. Actually, these undesirable rich space harmonics also make a big contribution to the torque ripple which could be harmful to the gear box in the large-scale wind turbines [8]. As already indicated in [8], the largest contribution to the torque ripple of the case study machine was because of the winding distribution space-harmonics. The slotting effect has some contribution to the torque ripple while the influence of the induced time-harmonic rotor currents on the torque ripple is negligible.

Skew is quite practical to reduce the torque ripple and it will also result in an induced rotor currents with less time-harmonics [9], [10]. It has been proven analytically that the torque ripple of BDFIM decreases by rotor skew [11]. The slotting effect of stator slots and the saturation are ignored in that analytical model while they two may also have some influence on the torque ripple. In addition, it is also assumed that the nested-loop rotor has only one loop per nest and its slot are rectangular shaped. But it is already shown that the number of loops per nest has an effect on the torque ripple [12]. Finite element (FE) model can overcome these assumptions since it can easily to take into account the exact geometry and the saturation effect. It is already applied in the brushless doubly-fed reluctance machine [13], but not yet in the BDFIM. This paper uses a transient 2D FE model with multi-slice method [10], [13] to investigate the effects of the rotor skew on the torque ripple, as well as the copper and core losses, in the case without and with saturation.

The aim of this paper is to apply 2D multi-slice FE method to study the effect of rotor skew on the performance of the BDFIM. This paper starts with the FE modeling of

The research leading to these results has received funding from the European Union's Seventh Framework Programme managed by REA - Research Executive Agency (FP7/2007_2013) under Grant Agreement N.315485.

The research leading to these results has received funding from the China Scholarship Council for supporting X. Wang's PhD research work.

X. Wang, T. D. Strous, H. Polinder and J. A. Ferreira are with the Department of Electrical Sustainable Energy, Delft University of Technology, Delft, The Netherlands, (email: X.Wang-3@tudelft.nl, T.D.Strous@tudelft.nl, H.Polinder@tudelft.nl, J.A.Ferreira@tudelft.nl).

D. Lahaye is with the Delft Institute of Applied Mathematics, Delft University of Technology, Delft, the Netherlands, (email: D.J.P.Lahaye@tudelft.nl).

978-1-4799-7940-0/15/$31.00 ©2015 IEEE

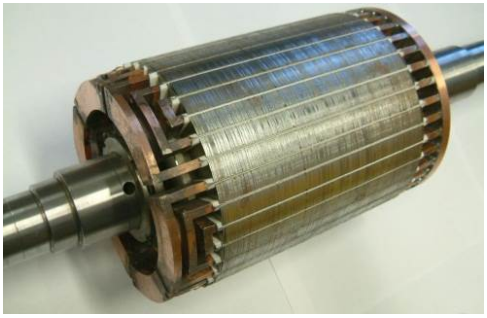

Fig. 1. Nested-loop structure of the BDFIM considered [2]

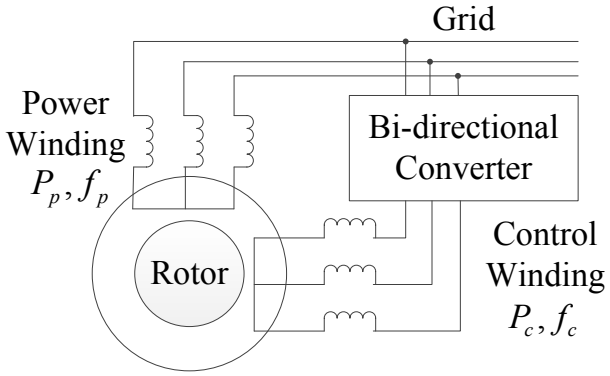

Fig. 2. The structure of the BDFIM

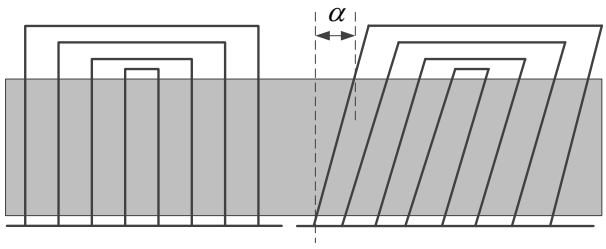

Fig. 3. Nested-loop rotor without & with skew

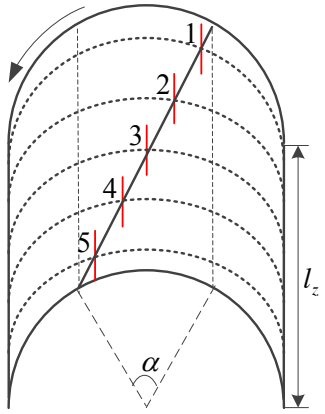

Fig. 4. Multi-slice representation of the rotor skew

rotor skew with multi-slice method. Next, the methods to calculated the rotor currents, electromagnetic torque and losses are introduced. Subsequently, the simulation results without rotor skew and with different skew angles are given in both cases without/with saturation, followed by a discussion on the results. Finally, conclusions are drawn.

II. Modeling of Rotor Skew

A. Assumptions

The following assumptions are made in this model:

1) The eddy-currents in the iron cores are neglected during the FE calculation while the core losses are computed in the post-processing. This is guaranteed because the eddy-currents are reduced significantly due to the lamination structure in the core.
2) The skin-effect and the proximity-effect are ignored for the stator windings and solid rotor bars. This will be investigated separately in the later paper.
3) The resistances of the end parts of the rotor bar are taken into account by coupling the electrical circuits with the FEM equations while the magnetic field due to the end part is neglected.

B. Transient FE model with Multi-Slice Method

The rotor bars are no longer parallel to the axial direction since the bar is skewed with an angle. Therefore, the rotor skew is essentially a 3D problem due to the fact that the induced rotor currents do not flow only along the axial direction. However, one approximate way is to represent a skewed machine with a 2D FE model with multi-slice method [10], [13]. The nested-loop rotor with skew angle α is shown in Fig. 3 and Fig. 4 gives the representation of the skew by using multi-slice method. The currents in each slice are assumed to flow only in the axial direction. Therefore, a set of normal 2D models is used to model the skewed rotor. Each slice corresponds to a section with l_z/m length which taken at different positions along the axial direction, where m is the number of the slices. This can be achieved by making the relative position between the stator and the rotor of the middle slice (e.g. No. 3 in Fig. 4) correspond to that of the machine without skewed rotor and the other slices are shifted with $\pm\alpha/m$ angle one by one (shown in Fig. 4). The 2D electromagnetic field equation in each slice is solved simultaneously as:

$$\frac{\partial}{\partial x}(\frac{1}{\mu}\frac{\partial A_z^n}{\partial x}) + \frac{\partial}{\partial y}(\frac{1}{\mu}\frac{\partial A_z^n}{\partial y}) = J_{e,z}^n, \tag{1}$$

where n represents the label number of the slice ($n = 1, 2, .., m$), μ is the permeability of the material, A_z is the z component of the magnetic vector potential and J_e, z is the externally applied current density. The rotor rotation is modeled by using Arbitrary Lagrangian-Eulerian (ALE) formulation. Each slice is meshed separately. One constrain is enforced to obtain the same current in corresponding rotor bar of each slice. This leads to the circuit equation (2) which will be coupled to related the unknown rotor current I_r with

the resultant magnetic field:

$$\frac{l_z/m}{S}\sum_{n=1}^{n=m}\frac{d(\iint A_z^n dS_+ - \iint A_z^n dS_-)}{dt} - I_r R = 0, \quad (2)$$

where l_z is the axial length, S is the cross-sectional area of the rotor bar, S_+ and S_- are the surface of the go and return conductors, R is the resistance of one rotor loop including the resistance of the end parts of the bar. The skew angle α is relatively small in practical application. The components of the rotor currents in axial direction dominate in total. Therefore, the flux in axial direction is neglected in our model.

C. Electromagnetic Torque, Torque Ripple and Losses

Maxwell's stress tensor method is used for the toque calculation in each slice. The torque with skewed rotor is:

$$T_e = \sum_{n=1}^{n=m}\frac{l_{stk/m}}{\mu_0}\int_0^{2\pi} r^2 B_r^n B_t^n d\theta, \quad (3)$$

where μ_0 is the permeability of the vacuum, r is the radius of the air-gap, B_r and B_t are the radial and tangential components of the flux density in the air-gap. The torque ripple is defined as:

$$ripple = \frac{max(T_e) - min(T_e)}{average(T_e)} \times 100\%. \quad (4)$$

The calculation of the copper losses is straightforward and the core losses can be evaluated by Modified Steinmetz Equation (MSE) [14]. The detailed equations of the losses calculation and the specifications of the electric steel used in the core can be found in the FE modeling of BDFIM [15].

III. Results and Discussion

The main specifications of the BDFIM simulated are given in Table. I. In order to show the influence of the saturation, all the results given in this section are without and with saturation. However, the simulation results of the model without saturation is actually too far from the reality.

Fig. 5 shows the induced rotor currents in the most outer loop in the case without and with saturation. The saturation

TABLE I
Main Specifications of the BDFIM Studied

Description	Machine parameter	Value
Axial length [m]	l_{stk}	1.596
Air-gap length [mm]	l_g	1.5
Stator outer radius [m]	r_{so}	0.83
Stator inner radius [m]	r_{si}	0.67
Rotor inner radius [m]	r_{ri}	0.58
Number of phases	N_{ph}	3
Number of pole-pairs	p_p, p_c	4, 6
Rated frequency [Hz]	f_p, f_c	50, 10
Number of stator slots	N_{ss}	72
Number of rotor nests	N_{nest}	10
Number of loops per nest	q_r	4
Rotational speed [rad/s]	ω_m	37.7
Rated power [MW]	P	3.0

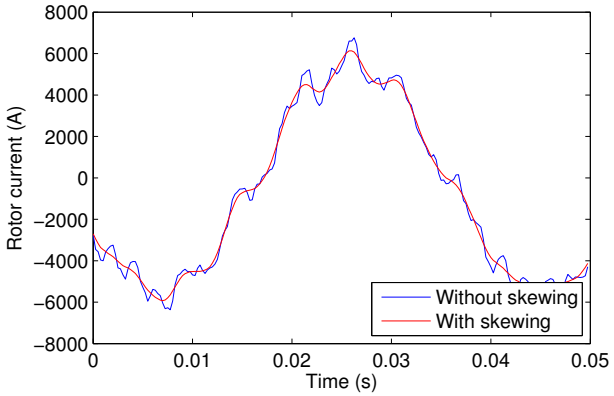

(a) Without saturation

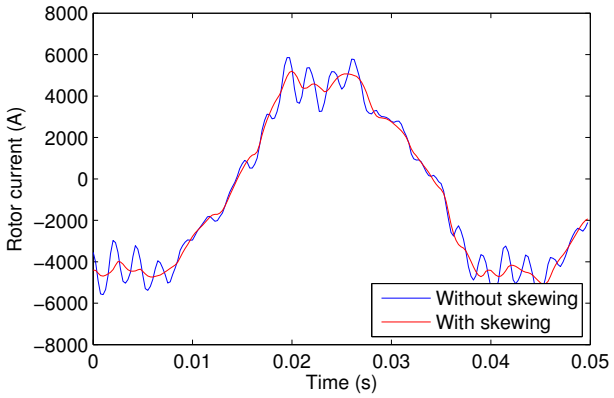

(b) With saturation

Fig. 5. Induced rotor currents in the most outer loop

leads to more time-harmonics in the rotor currents. The time-harmonics are reduced in the rotor current by applying rotor skew. This could also help to reduce the torque ripple although [8] indicates the effect of induced time-harmonic rotor currents on the torque ripple is much smaller comparing with the winding distribution and the slotting space-harmonics.

Fig. 6 and Fig. 7 give the torque response in the case without saturation and with saturation, respectively. The torque shown in Fig. 6 achieves an unrealistic high level because the saturation is ignored. However, the torque ripples of both cases are reduced by applying the rotor skew.

Fig. 8 and Fig. 9 show the time FFT results of the torque responses shown in Fig. 6(a) and Fig. 7(a). It is found that the saturation results in more harmonics in the spectrum comparing Fig. 8 and Fig. 9. And those harmonics are hardly influenced by the rotor skew comparing Fig. 9(a) and (b). In addition, the second largest component in the spectrum is 380 Hz in the non-skew cases (shown in Fig. 8(a) and Fig. 9(a)). This component is caused by the winding distribution and the slotting space-harmonics [8]. They are reduced effectively by the rotor skew both in linear and saturation situations.

Fig. 10 summaries the average torque and the torque ripple with respect to different skew angles. It seems one stator slot pitch τ_s would be a compromise choice for the skew angle in the BDFIM studied because the ripple is reduced significantly while the average torque does not significantly decrease. This

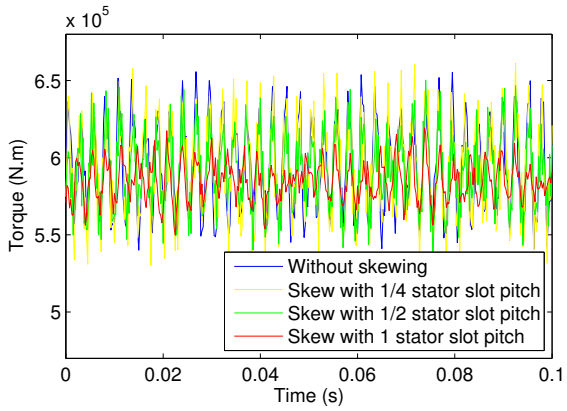

(a) All view

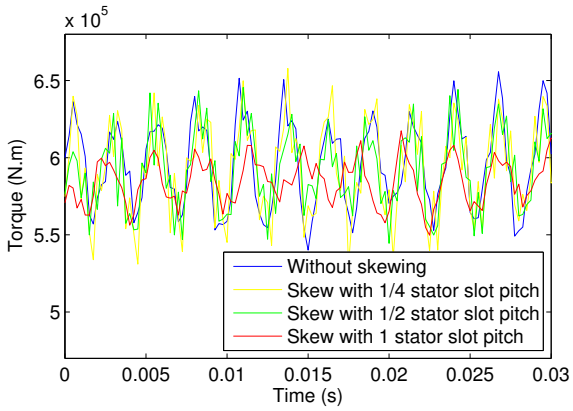

(b) Enlarged view

Fig. 6. Torque response without saturation

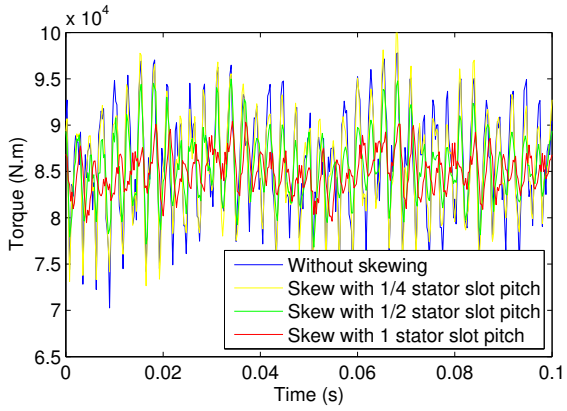

(a) All view

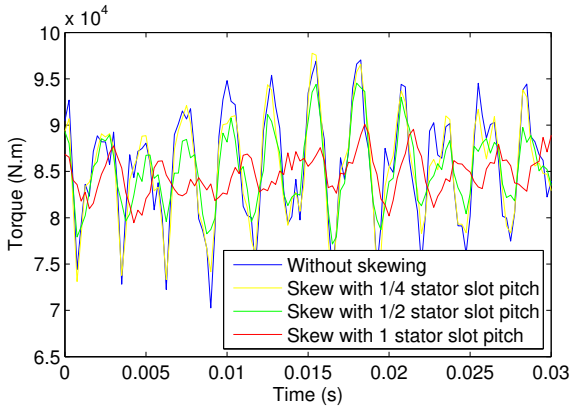

(b) Enlarged view

Fig. 7. Torque response with saturation

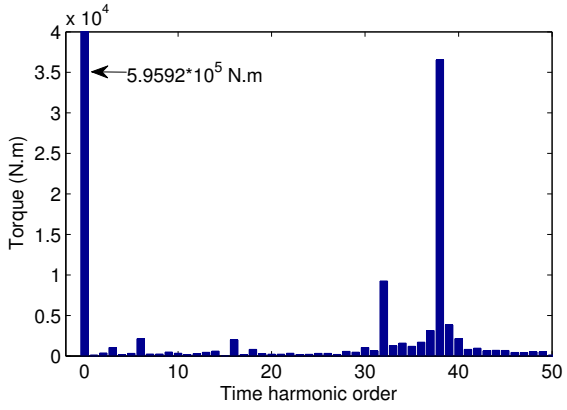

(a) Without skew

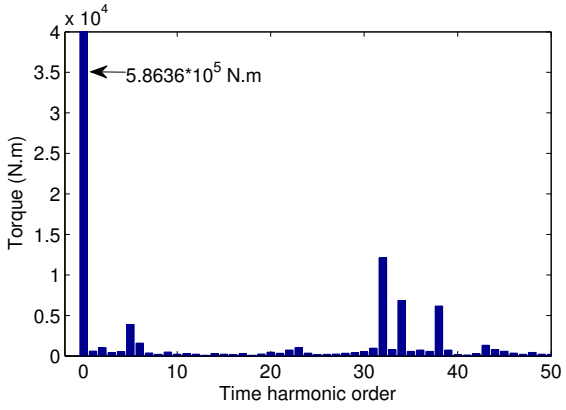

(b) Skew with 1 stator slot pitch

Fig. 8. Time FFT analysis of the torque response without saturation

choice is also practical in common squirrel-cage induction machines. However, more points should be simulated to get the exact angle for the minimum torque ripple. It because the torque ripple depends on a lot of factors and there is no unified skew angle for a certain kind of machine.

Table. II gives the losses of the BDFIM considering saturation. Without skewing, the core losses corresponding to $l_z/5$ length are the total core losses divided by five. In the case with rotor skew, the core losses due to the flux in the axial direction are not considered. Each slice corresponds to a 2D model with $l_z/5$ length, but with $\alpha/5$ angle shifted. According to the characteristic of the torque with respect to the relative position between the stator and the rotor shown in Fig. 11, different slice actually corresponds to a different operation point. This

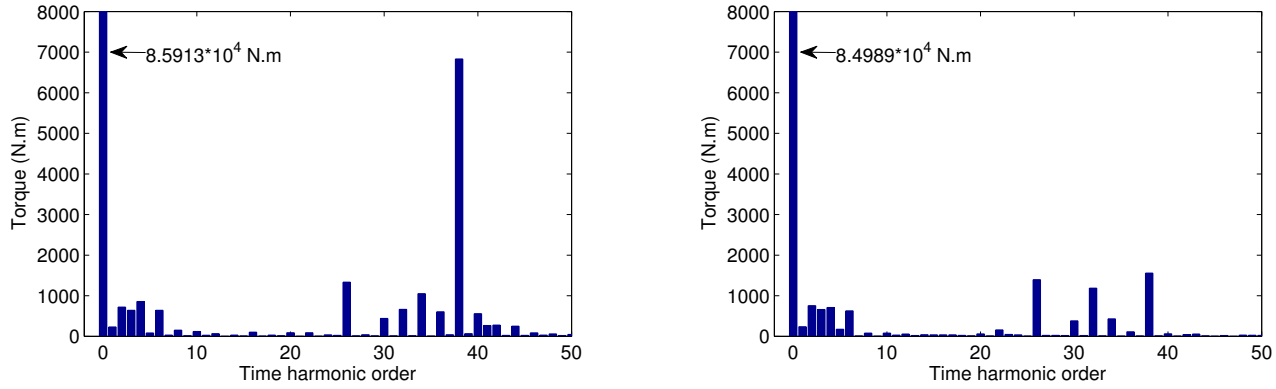

(a) Without skew (b) Skew with 1 stator slot pitch

Fig. 9. Time FFT analysis of the torque response with saturation

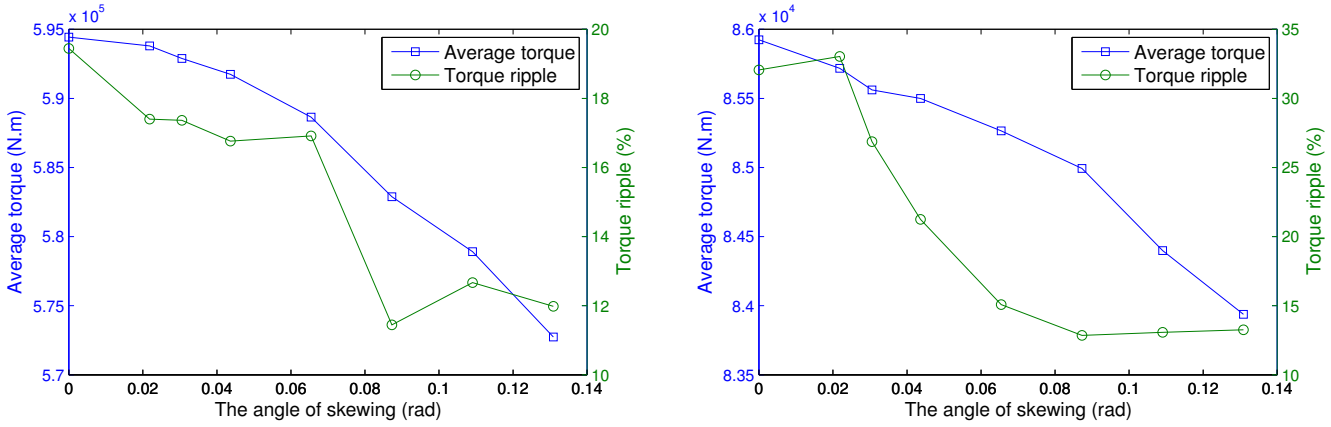

(a) Without saturation (b) With saturation

Fig. 10. Comparison of average torque and torque ripple with respect to different skew angles

TABLE II
PERFORMANCE OF BDFIM WITH DIFFERENT SKEW ANGLES CONSIDERING SATURATION

Performance		**Stator core losses P^s_{core} [kW]**						**Rotor core losses P^r_{core} [kW]**						P^r_{Cu}
Slice No.		**1**	**2**	**3**	**4**	**5**	**Total**	**1**	**2**	**3**	**4**	**5**	**Total**	**[kW]**
Skew angle [rad]	0	13.45	13.45	13.45	13.45	13.45	67.25	3.83	3.83	3.83	3.83	3.83	19.15	33.84
	$0.25\tau_s$	13.52	13.46	13.40	13.34	13.28	67.00	3.86	3.84	3.83	3.81	3.79	19.13	33.64
	$0.35\tau_s$	13.64	13.49	13.40	13.32	13.24	67.10	3.88	3.85	3.83	3.80	3.78	19.13	33.46
	$0.50\tau_s$	13.68	13.54	13.42	13.30	13.19	67.12	3.90	3.86	3.83	3.79	3.76	19.13	33.18
	$0.75\tau_s$	13.92	13.63	13.43	13.26	13.09	67.33	3.94	3.88	3.82	3.77	3.72	19.14	32.76
	$1.00\tau_s$	14.05	13.72	13.45	13.21	13.01	67.43	3.99	3.90	3.82	3.76	3.70	19.16	32.52
	$1.25\tau_s$	14.27	13.81	13.45	13.16	12.93	67.62	4.05	3.92	3.81	3.74	3.68	19.19	32.47
	$1.50\tau_s$	14.37	13.89	13.46	13.11	12.84	67.67	4.10	3.94	3.80	3.72	3.66	19.23	32.53

results in the difference of the core losses in different slices. This difference becomes bigger with the skew angle increases. Actually, this phenomenon of the core losses redistribution is also observed in common induction machine with skewed squirrel-cage rotor [9]. However, the rotor skew has little effect on the total amount of core losses. In addition, the rotor copper losses decrease with the skew angle increases (up to $1.25\tau_s$ in the case study). It because the time-harmonics of the rotor currents are reduced by applying the rotor skew. Fig. 11 shows the BDFIM characteristic resembles the torque load-angle characteristic of synchronous AC machines. It means the BDFIM can operate as a synchronous machine.

IV. CONCLUSION

This paper applies a 2D multi-slice FE model to study the influence of the rotor skew on the performance of the

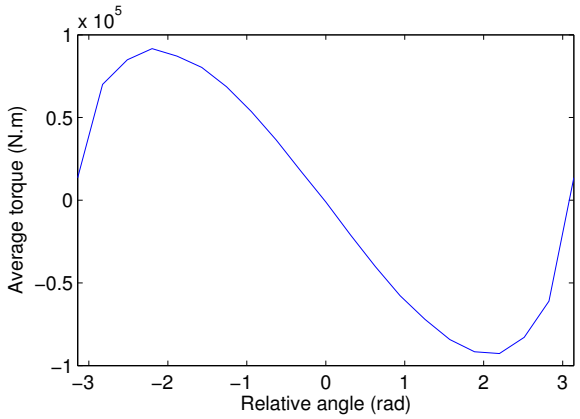

Fig. 11. Torque characteristic as function of relative position between the stator and the rotor with saturation

BDFIM considered. The results indicate that the largest component for torque ripple due to the space-harmonics of the winding distribution and the slotting is reduced significantly by applying the rotor skew. The rotor skew has negligible influence on the space-harmonics due to the saturation. One stator slot pitch can be a compromise choice for rotor skew angle considering the average torque and the torque ripple. The induced rotor currents result in less time-harmonics with skewed rotor. Furthermore, the rotor skew has little effect on the total amount of losses. But the core losses redistribute along the axial direction. This might require attention in the design of the cooling system.

REFERENCES

[1] H. Polinder, *Overview of and Trends in Wind Turbine Generator Systems*, Proceedings of the IEEE Power and Energy Society General Meeting, Jul. 2011.

[2] H. Polinder, J. A. Ferreira, B. B. Jensen, A. B. Abrahamsen, K. Atallah and R. A. McMahon, *Trends in Wind Turbine Generator Systems*, IEEE Journal of Emerging and Selected Topics in Power Electronics, vol.1, no.3, Sept. 2013.

[3] T. Long, S. Shao, D. Abdi, R. A. McMahon, S. Liu, *Asymmetrical Low-Voltage Ride Through of Brushless Doubly Fed Induction Generator for the Wind Power Generation*, IEEE Trans. on Energy Conversion, vol.28, no.3, pp.502-511, Sept. 2013.

[4] E. Abdi, M. R. Tatlow, R. A. McMahon and P. Tavner, *Design and Performance Analysis of a 6MW Medium-Speed Brushless DFIG*, Renewable Power Generation Conference (RPG 2013), 2nd IET, Sept. 2013.

[5] R. A. McMahon, X. Wang, E. Abdi-Jalebi, P. J. Tavner, P. C. Roberts, and M. Jagiela, *The BDFM as a Generator in Wind Turbines*, in Power Electronics and Motion Control Conference, 2006. EPE-PEMC 2006. 12th International, Sept. 2006.

[6] R. A. McMahon, P. C. Roberts, X. Wang and P. J. Tavner, *Performance of BDFM as Generator and Motor*, IEE Proc. Electr. Power Appl., vol.153, no.2, pp.289-299, Mar. 2006.

[7] T. D. Strous, N. H. van der Blij, H. Polinder and J. A. Ferreira, *Brushless Doubly-Fed Induction Machines: Magnetic Field Modelling*, XXI International Conference on Electrical Machines(ICEM'2014), Berlin, Germany, Sept. 2014.

[8] T. D. Strous, Xuezhou Wang, H. Polinder and J. A. Ferreira, *Brushless Doubly-Fed Induction Machines: Torque Ripple*, Electric Machines & Drives Conference (IEMDC), 2015 IEEE International, Coeur d'Alene, USA, May. 2015, to be published.

[9] Y. Kawase, T. Yamaguchi, Z. Tu, N. Toida, N. Minoshima and K. Hashimoto, *Effects of Skew Angle of Rotor in Squirrel-Cage Induction Motor on Torque and Loss Characteristics*, IEEE Trans. on Magnetics, vol.45, no.3, March 2009.

[10] S. L. Ho and W. N. Fu, *A Comparehensive Approach to the Solution of Direct-Couple Multislice Model of Skewed Rotor Induction Motors Using Time-Stepping Eddy-Current Finite Element Method*, IEEE Trans. on Magnetics, vol.33, no.3, May 1998.

[11] H. Gorginpour, B. Jandaghi, A. Oraee, M. A. Saket, M. Ahmadian and H. Oraee, *Reduction of the Torque Ripple in Brushless Doubly-Fed MAchine*, Proceedings of the 2011 3rd International Youth Conference on Energetics (IYCE), 2011.

[12] N. H. van der Blij, T. D. Strous, Xuezhou Wang and H. Polinder, *A Novel Analytical Approach and Finite Element Modelling of a BDFIM*, XXI International Conference on Electrical Machines(ICEM'2014), Berlin, Germany, Sept. 2014.

[13] D. G. Dorrell, A. .M. Knight and R. E. Betz, *Issues with the Design of Brushless Doubly-Fed Reluctance Machines: Unbalanced Magnetic Pull, Skew and Iron Losses*, Electric Machines & Drives Conference (IEMDC), 2011 IEEE International, May 2011.

[14] H. Gorginpoer, H. Oraee and E. Abdi, *Calculation of Core and Stray Load Losses in Brushless Doubly Fed Induction Generators*, IEEE Trans. on Industrial Electronics, vol.61, no.7, Jul. 2014.

[15] Xuezhou Wang, T. D. Strous, D. Lahaye, H. Polinder and J. A. Ferreira, *Finite Element Modeling of Brushless Doubly-Fed Induction Machine (BDFIM) Based on Magneto-Static Simulation*, Electric Machines & Drives Conference (IEMDC), 2015 IEEE International, Coeur d'Alene, USA, May. 2015, to be published.

V. BIOGRAPHIES

Xuezhou Wang received the M.Sc. degree in power electronics and electrical drives from Northwestern Polytechnical University, Xi'an, China, in 2013. Currently, he is working towards his Ph.D. degree in the field of electrical machines. His current research interests include numerical modeling and design of electrical machines.

Tim D. Strous received the M.Sc. degree in electrical engineering from Delft University of Technology, Delft, The Netherlands, in 2010. Currently, he is working towards the Ph.D. degree in the field of electrical machines. His current research interests include modeling and design of electrical machines and drives.

Domenico Lahaye received the M.Sc. degree in applied mathematics from the Free University of Brussels, Brussels, Belgium, in 1994, the postgraduate degree in mathematics from the Eindhoven University of Technology, Eindhoven, The Netherlands, in 1996, and the Ph.D. degree in computer science from the Katholic University of Leuven, Leuven, Belgium, in 2001. After having held positions at the Center for Advanced Studies, Research and Development in Sardinia and at the National Research Center for Mathematics and Computer Science in The Netherlands, he joined the Numerical Analysis Research Group, Delft Institute of Applied Mathematics, Delft University of Technology, Delft, The Netherlands, in 2007.

Henk Polinder received the MSc and the PhD degree from Delft University of Technology, Delft, The Netherlands, in 1992 and 1998. Since 1996 he has been an assistant/associate professor in the Electrical Power Processing Group of Delft University of Technology. He worked part-time at Lagerwey in Barneveld in 1998/1999, at Philips Applied Technologies in Eindhoven in 2002 and at ABB Corporate Research in Vasteras in 2008. He was a visiting professor at the University of Newcastle-upon-Tyne in 2002, at Laval University, Quebec in 2004 and at the University of Edinburgh in 2006. He is author or coauthor of over 200 papers. His research interests include design aspects of electrical machines, mainly for renewable energy applications.

Jan A. Ferreira received the B.Sc.Eng., M.Sc..Eng., and Ph.D. degrees in Electrical Engineering from the Rand Afrikaans University, Johannesburg, South Africa in 1981, 1983 and 1988 respectively. In 1981 he was with the Institute of Power Electronics and Electric Drives, Technical University of Aachen, and worked in industry at ESD (Pty) Ltd from 1982-1985. From 1986 until 1997 he was at the Faculty of Engineering, Rand Afrikaans University, where he held the Carl and Emily Fuchs Chair of Power Electronics in later years. Since 1998 he is a professor at the Delft University of Technology in The Netherlands. Dr. Ferreira is a fellow of the IEEE.